Journal of Power Sources 196 (2011) 8714–8718

Contents lists available at ScienceDirect

Journal of Power Sources

journal homepage: www.elsevier.com/locate/jpowsour

Short communication

Formulation and characterization of ultra-thick electrodes for high energy lithium-ion batteries employing tailored metal foams

John S. Wang[a,*], Ping Liu[a], Elena Sherman[a], Mark Verbrugge[b], Harshad Tataria[c]

[a] Sensors and Materials Lab, HRL Laboratories LLC, United States
[b] Chemical Sciences and Materials Systems Lab, General Motors R&D, United States
[c] Battery Systems Engineering, General Motors Vehicle Engineering, United States

ARTICLE INFO

Article history:
Received 1 June 2011
Received in revised form 21 June 2011
Accepted 21 June 2011
Available online 28 June 2011

Keywords:
Thick electrode
3D electrode
Metal foam
Current collector
Cu foam electrode
Al foam electrode

ABSTRACT

Increasing the thickness of a battery electrode without comprising cell electrochemical performance, such as power density and cycling stability, is very challenging. In this work, we demonstrate the utility of 3D (three dimensional) Cu foam framework as a current collector for building carbon negative electrodes as thick as 1.2 mm. When tested in a bipolar configuration, electrodes of 1.2 and 0.6 mm thick delivered capacities of over 350 mAh g^{-1} (>95% of theoretical capacity) up to a C/5 rate. We have also assembled a full cell composed of a 1.2 mm thick negative electrode with Cu foam as the current collector and a 1.2 mm thick L333 ($LiNi_{1/3}Mn_{1/3}Co_{1/3}O_2$) positive electrode with Al foam as the current collector. The cell exhibited good capacity retention at low rates. These results underscore the promise of 3D foam structures in terms of enabling ultra-thick electrodes for high energy density battery applications.

1. Introduction

Particularly for traction applications, it is necessary to reduce the cost, size, and volume, of lithium ion batteries. In addition to searching for cathode (positive electrode) and anode (negative electrode) materials with higher capacities, there is also a need to improve the battery cell design to maximize energy density [1,2]. Specifically, current state of the art (SOA) batteries realize less than 1/3 of their theoretical energy density in part due to the large amount of inactive components in the cells, such as outer packaging, current collectors, separators, and electrolytes. For the Chevy Volt, a so called 3P96S configuration is employed. That is, each cell unit (45 Ah and about 3.7 V at 50% state of charge) has 3 cells (each of 15 Ah) attached in parallel (hence, 3P), and 96 such cell units are connected in series (hence, 96S, yielding a 355 V pack at 50% state of charge). The 3P design, as compared to an 1P, adds complexity and cost of system monitoring and control and reduces effective system energy density.

A potential approach to reduce inactive components in battery cells is to increase the thickness of the electrode coating. This approach also leads to fewer welds needed to otherwise join the cells to be connected in parallel. Currently, electrode layer thicknesses are in the range of 50–100 μm. It is common practice to reduce layer thickness to increase cell power density, which comes at the price of reduced energy density, as there is more current collector per unit mass of active material. A major factor affecting the power density of battery electrodes is their electronic conductivity. Conceivably, if a 3D current collector could be constructed so that all particles are not more than 50–100 μm from the nearest current collector, and the electrode material housing the particles (including binders and conductive diluents) is similar to that which is used today, then thicker electrodes could be realized without a major loss in power as determined by, for example, a 10-s power test [3]. Examples of 3D current collectors include carbon fiber or nanotube forests grown on metal current collectors, vertically aligned graphene sheets, porous or patterned metals, and carbon and metal foams [4–22]. Our current work focuses on metal foams since they are the most suitable to use the slurry coating process to fabricate electrodes and are likely to be the least expensive option relative to those referenced. While not addressed in this work, a potential risk associated with the use of metal foam current collectors is cell shorting, as the metal foam could poke through the polymeric separator more easily that a smooth, solvent cast conventional electrode. Another potential issue that must be considered in the electrode formulation is that calendering (physical pressing) of the electrode material (e.g., binder, active material, and conductive diluents) to the current collector is not easily accomplished with a foam current collector.

* Corresponding author. Tel.: +1 310 317 5155; fax: +1 310 317 5840.
E-mail address: jswang@hrl.com (J.S. Wang).

0378-7753/$ – see front matter © 2011 Published by Elsevier B.V.
doi:10.1016/j.jpowsour.2011.06.071

We will first describe the electrochemical performance of the Cu foam as a current collector for the graphite negative electrode. We prepared Cu foam electrodes with two thicknesses: 1.2 and 0.6 mm. Both thicknesses far exceed those normally employed. Next, we designed a bipolar cell so as to reduce the effective cell thickness by one half. We shall investigate and compare the electrochemical performance of Cu foam electrodes at three different thicknesses: 1.2, 0.6 and 0.3 mm, and we examine an ultra-thick L333 cathode electrode using Al foam as a current collector. Last, we show experimental data for a full cell composed of a Cu foam graphite negative and Al foam L333 positive electrode. Using galvanostatic charge/discharge method, we investigate the lithium ion storage capacities, cycling stabilities, and rate capabilities. Overall, the results lend support to the use of 3D structured foam as current collectors enabling ultra-thick battery electrodes and providing an effective approach to improve the active materials loading for high energy battery applications.

2. Experimental

2.1. Electrode preparation

Copper and aluminum foams were used as the current collectors for the negative and positive electrode. Both foam electrodes were filled using a slurry technique. Fig. 1 shows the images of Cu and Al foam architectures and their respective active material loadings. The as-received Cu foam (from E-foam) was about 1.2 mm thick with a porosity of 97%. The areal weight was 372 g m^{-2} (equivalent to 40 μm thick Cu foil). To study the effect of foam electrode thickness on the electrochemical performance, we reduced the foam thickness using a mechanical thinning technique. Briefly, the foam was first filled with a wax and then mechanically polished to a desired thickness, followed by removal of the wax. The thickness was reduced to 0.6 mm, with an areal weight of 188 g m^{-2}. The negative electrodes (Fig. 1B) were made using graphitic carbon as the active material. The composition was 93 wt% active carbon material (SG, Superior Graphite, SLC 1520), 3 wt% carbon black (Super P), and 4 wt% SBR binder (an aqueous styrene–butadiene rubber binder, LHB-108P). The active material loadings were 50–60 mg cm^{-2} for the 1.2 mm foam and 25–30 mg cm^{-2} for the 0.6 mm foam, respectively. Al foam was an ERG Duocel® foam (Fig. 1C), which comprises about 40 pores per inch (40 PPI). The foam was mechanically sliced to a desire thickness of 1.2 mm. The cathode materials were filled into the Al foam using a slurry composed of 84 wt.% $Li(NiCoMn)_{1/3}O_2$ (L333, NCM-01ST-5, Toda Kogyo) + 9 wt.% poly(vinylidene fluride-co-hexafluropropylene) binder (Kynar Flex 2801, Elf Atochem) + 3.5 wt.% carbon black (Super P, MMM) + 3.5 wt.% synthetic graphite (KS6, Timcal).

2.2. Characterization methods

The Cu foam half-cell electrochemical experiments were carried out in Swagelok cells inside an Argon filled glovebox. Two different types of Swagelok cells were used to investigate thickness effects. In addition to the traditional two-electrode cell, we designed a bipolar cell with one working electrode sandwiched by two counter electrodes. A schematic of the bipolar Swagelok cell is shown in Fig. 2. The bipolar cell design enables a reduction in the effective thickness of the working electrode by one half and represents how these electrodes could be used in a multilayer lithium ion stacked prismatic cell. For the half-cell testing, lithium metal was used as the counter electrode. The electrolyte solution was 1 M $LiPF_6$ in 1:1 (v/v) ratio ethylene carbonate (EC) to dimethyl carbonate (DMC). A Celgard 3501 (25 μm thick microporous polypropylene film with

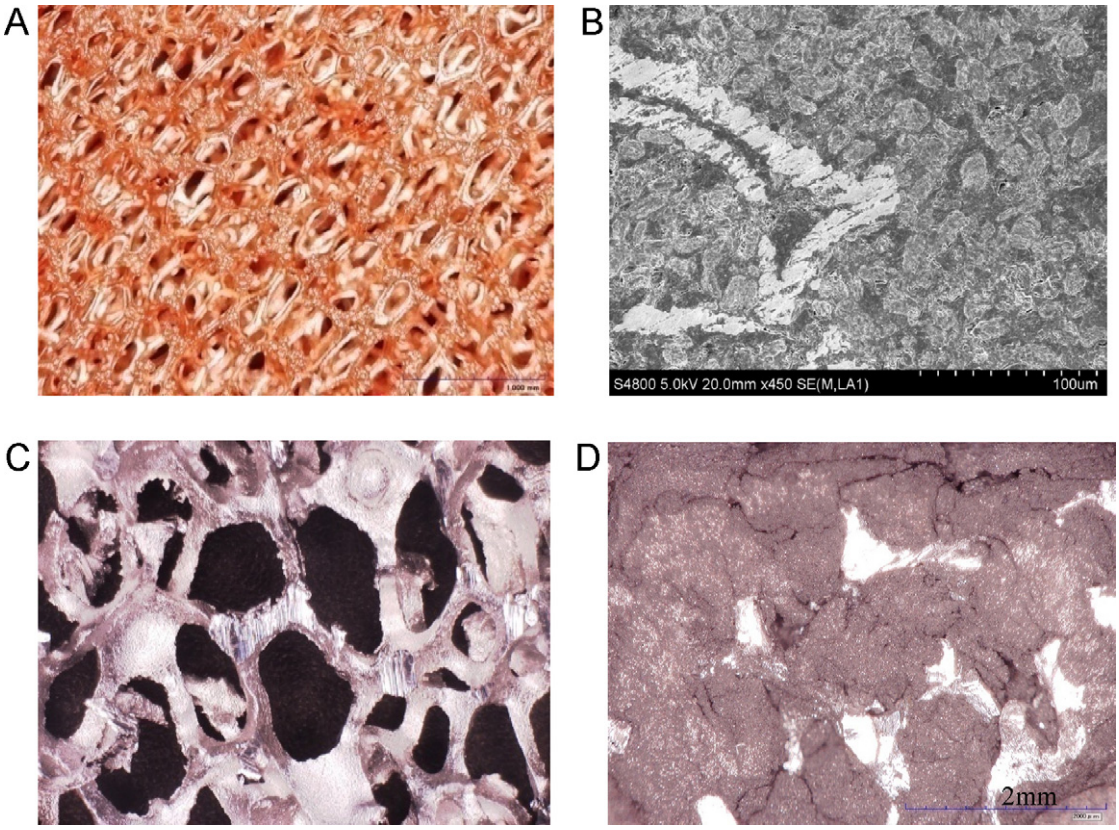

Fig. 1. Images of 3D foam structures and prepared electrodes. (A) Cu foam as a current collector for negative electrode; (B) graphite negative electrode using Cu foam; (C) Al foam as a positive current collector; and (D) L333 positive electrode using Al foam.

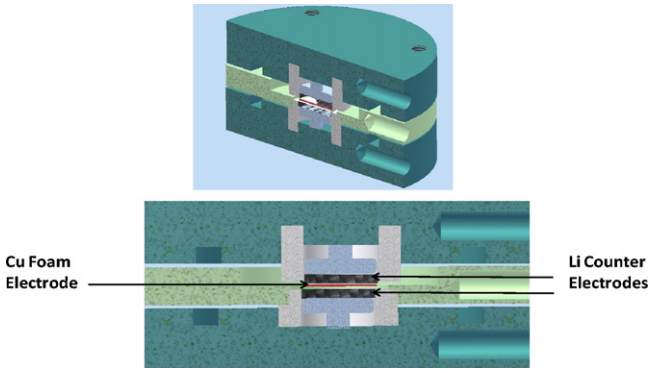

Fig. 2. Schematic of a bipolar cell setup. The Cu foam with graphite is the working electrode that is sandwiched by two lithium metal counter electrodes.

40% porosity) was used as the separator. A full cell composed of a Cu foam negative electrode and an Al foam positive electrode was assembled in a 2032 (20 mm in diameter and 3.2 mm in thickness) coin cell. Galvanostatic studies were performed on an Arbin BT-2000 battery testing station. The cycling voltage ranged from 10 mV to 2 V vs. Li for the Cu foam electrodes, and 3.2–4.3 V for the full cell systems.

3. Results and discussion

3.1. Electrochemical performance of Cu foam negative electrodes

Four different experiments were carried out using two Swagelok cell designs (unipolar and bipolar) on two electrode thicknesses (1.2 mm and 0.6 mm). While the traditional unipolar Swagelok cell allows us to investigate 1.2 and 0.6 mm thick samples, the bipolar cells can reduce their effective thickness down to 0.6 and 0.3 mm, respectively. We did find that (results not shown) the electrochemical performance of 1.2 mm thick samples using bipolar cells were very similar to those of the 0.6 mm thick samples using unipolar cells. The results further confirm that the bipolar cell design can effectively reduce the sample thickness by one half. In the following sections, we describe in detail three experiments to investigate the influence of the Cu foam thicknesses on electrochemical performance: (1) Sample A, unipolar cell test on a 1.2 mm thick sample; (2) Sample B, a bipolar cell test on a 1.2 mm thick sample; and (3) Sample C, a bipolar cell test on 0.6 mm thick sample.

Fig. 3a shows the charge/discharge characteristics of a 1.2 mm thick Cu foam negative electrode at C/20 and C/5 rates using a unipolar cell setup (Sample A). At a C/20 rate, the reversible charge capacity of this Cu foam graphite electrode was 345 mAh g^{-1}, about 93% of its theoretical capacity, 372 mAh g^{-1}. The active material loading on this sample was 50 mg cm^{-2}. The area-normalized capacity is more than 10 times higher than the current state-of-art battery electrodes. However, at a higher rate (C/5), the cycling stability was very poor (inset of Fig. 3a). This is mainly due to the impedance of the electrode. As shown in Fig. 3a, the voltage hysteresis between the charge and discharge rates of C/5 was much higher than those of the C/20 rate. In addition, the disappearance of the detailed voltage features of staging phenomenon in lithium graphite intercalation compounds further indicated that the overall kinetics were sluggish due to the high electrode impedance.

A major benefit of a bipolar cell is to effectively reduce the thickness of the Cu foam, nominally by one half. Since the current SOA battery electrodes are made of double-sided films supported by a current collector, the bipolar cell design allows us to investigate the performance of the electrode under conditions analogous to an SOA battery. Fig. 3b shows the charge/discharge characteristics of a 1.2 mm thick Cu foam negative electrode at C/15 and C/5 rates using a bipolar cell setup (Sample B). The inset of Fig. 3b illustrates its charge/discharge rate capabilities at C/15, C/5, and C/2. The active material loading for the sample was 60 mg cm^{-2}; relative to the bipolar configuration, the effective material loading was 30 mg cm^{-2} with an effective foam thickness of 0.6 mm. At both C/15 and C/5 rates, the specific capacity was over 350 mAh g^{-1}, close

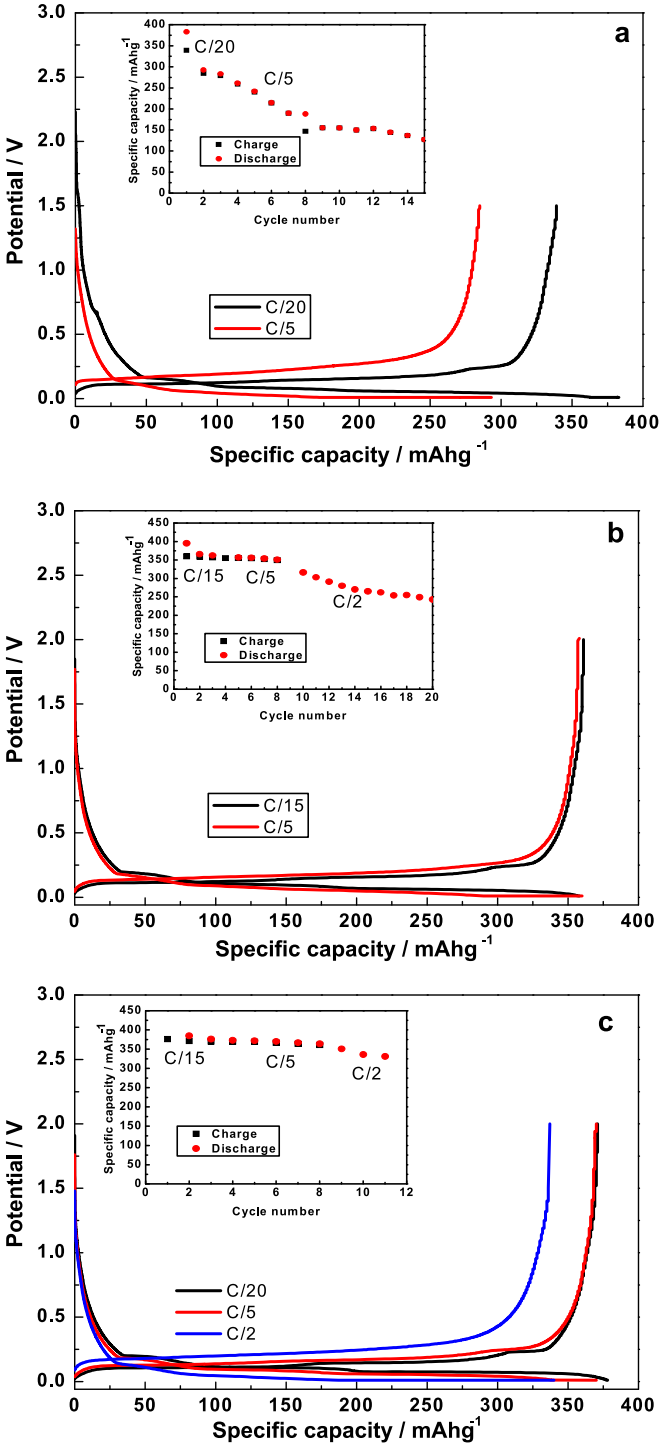

Fig. 3. Galvanostatic charge/discharge curves of Cu foam graphite electrode cycled: (a) 1.2 mm thick electrode C/20 and C/5 rates using the unipolar cell setup; (b) 1.2 mm thick electrode at C/15, C/5, and C/2 rates using the bipolar cell setup; (c) 0.6 mm at C/20, C/5, and C/2 rates using the bipolar cell setup. Insets: discharge capacity retention is plotted as a function of cycle number.

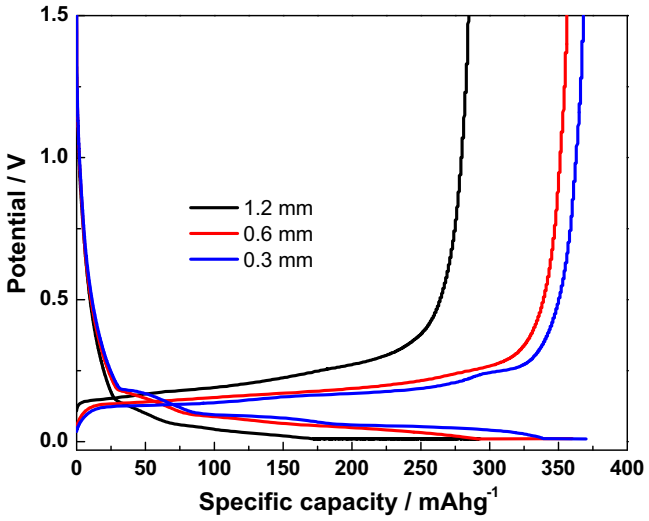

Fig. 4. A comparison of the charge/discharge behaviors of a Cu foam graphite electrode cycled at a C/5 rate for three different effective thicknesses: 1.2, 0.6, and 0.3 mm.

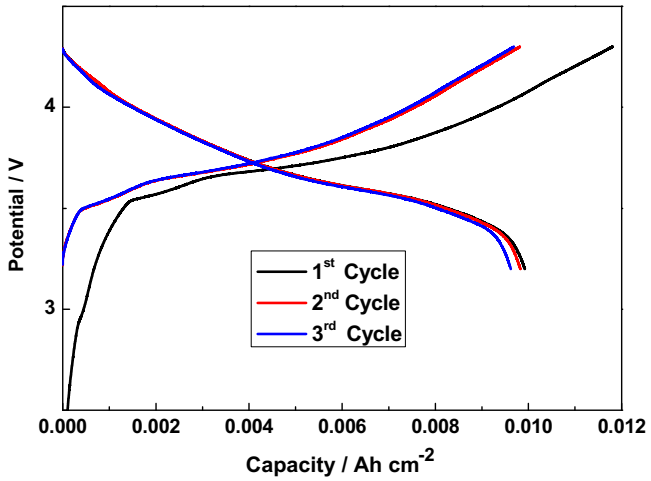

Fig. 5. Galvanostatic charge/discharge curves of a full cell composed of a 1.2 mm thick Cu foam graphite negative and 1.2 mm thick Al foam L333 positive electrode cycled at C/50 (1st of 3 cycles).

to 95% of the theoretical capacity. It is clearly indicated that, particularly at the C/5 rate, charge storage capacity was much higher than that of Sample A (shown in Fig. 3a). In addition, a much smaller voltage gap was observed between C/15 and C/5 rate for Sample B than Sample A, suggesting that the electrode was much less resistive due to the reduction of the effective thickness using the bipolar cell setup. The cycling stability (inset of Fig. 3b) was also significantly better than the prior sample. However, at the C/2 rate, the capacity fades quickly, due mainly to soft shorting during the charging process. Because of the large capacity per unit area, the current density on the lithium metal counter electrode is very high, which accelerates dendrite growth on lithium surface. Nonetheless, we have demonstrated that both the charge storage capability and cycling stability were significantly better for Sample B than Sample A, and we attribute this to the bipolar cell design, which reduces electrode resistance by reducing the effective thickness of the electrode in half.

For comparison, we have also examined the electrochemical performance of the 0.6 mm Cu foam electrode using a bipolar cell. Fig. 3c shows the charge/discharge characteristics at C/20, C/5, and C/2 rates (Sample C). The active material loading on this sample was 28 mg cm^{-2}; hence, the effective material loading is 14 mg cm^{-2} with an effective foam thickness of 0.3 mm. The initial capacity at the C/20 rate is very close to the theoretical capacity. A closer examination of the charge/discharge profiles reveals that detailed features of the multistage phase transitions of graphite are clearly visible and the plateau voltages are very close to the equilibrium voltage of the graphite [23]. This is a good indication that the resistance of the film was much less than the prior two samples. Even at a C/5 rate, the charge/discharge capacity was quite good, and good cycling stability was observed (inset of Fig. 3c). Again, the cycling performance at C/2 was poor due to lithium dendrite growth over the counter electrode.

The effects of electrode thickness on the electrochemical performance can be clearly seen by evaluating the charge/discharge characteristics under a constant rate. Fig. 4 shows a comparison of the galvanostatic charge/discharge curves at a C/5 rate for Samples A, B and C, with effective thicknesses of 1.2, 0.6, and 0.3 mm, respectively. As expected, for the same charge/discharge rate, the specific capacity is higher for the thinner electrode. In addition, the voltage hysteresis between the charge and discharge are smaller for the thinner electrode. The resistance of the electrode increases as the thickness increases. Overall, the results demonstrate that both 0.6 and 0.3 mm Cu foam electrodes exhibit promising storage capabilities with good cycling stabilities up to a C/5 rate. These results establish that the 3D structured current collectors can significantly improve the cycling performance of ultra-thick electrodes for high energy density batteries.

3.2. Full cell composed of Cu and Al foam electrodes

We have also investigated the performance of a full cell using the Cu foam negative electrode and Al foam positive electrode. The Al foam positive electrode is composed of a L333 active cathode material. A 2032 coin cell was assembled using these two foam electrodes. Both positive and negative electrodes are 1.2 mm thick. The active material loading of the graphite negative and L333 positive electrodes are 28 and 89 mg cm^{-2}, respectively the practical capacity of the graphite and L333 are about 360 and 140 mAh g^{-1}, respectively. When considering the initial formation cycle loss on graphite due to SEI formation, the storage capacities of these two electrodes are equally matched to good approximation. Fig. 5 shows the galvanostatic charge/discharge profiles of the first 3 cycles at a slow rate of C/50. Except for the 1st charging cycle, the charge/discharge behaviors were very similar for the first 3 cycles with very little capacity fade. By comparing the 1st charge cycle capacity with the capacity obtained from subsequent cycles, we estimated 20% lithium loss due to SEI formation during the initial formation cycle. After the initial loss, we were able to achieve 10 mAh cm^{-2} of reversible storage capacity. This corresponds to the storage capacities of 357 mAh g^{-1} for the graphite negative electrode and 112 mAh g^{-1} for the L333 positive electrode.

Fig. 6 (inset) shows a comparison of discharge capacities of the full cell at various rates: C/50, C/20, C/10, C/2.5, C/25, and C/5. Capacity fade was evident upon cycling, particularly, as expected, at higher rates. The results demonstrate that cycling stability at low rates is much better than that at higher rates. A closer examination of the charge/discharge profiles provides additional insight. Fig. 6 shows the charge/discharge curves of the full cell at different rates: C/50, C/20, C/5, and C/2.5. At C/50, the detailed voltage features of both graphite and L333 can be observed in the charge/discharge curves of the full cell. These results suggest that there is little kinetic limitation at such slow rates. As the rate increases, we see two effects: (1) the voltage hysteresis increases; and (2) the slope of the curves become steeper. Using the discharge event as an example (Fig. 6), we see that as the rate increases, the voltage profiles

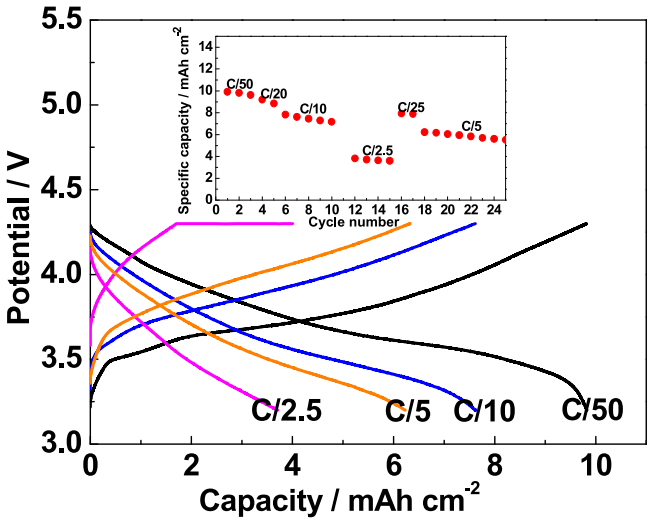

Fig. 6. A comparison of the charge/discharge behaviors of a full cell composed of a 1.2 mm thick Cu foam graphite negative and a 1.2 mm thick Al foam L333 positive electrode cycled at C/50, C/10, C/5, and C/2.5 rates. Inset: discharge capacity retention plotted as a function of cycle number at different rates.

shift downward; this phenomenon reflects the intrinsic resistance from the electrodes. The steeper slope of the voltage profiles with the increasing rates reveals that there are kinetic limitations.

4. Conclusion

In this report, we have presented the utility of 3D structured foam as the current collector geometry that enables ultra-thick electrodes for improved energy density of lithium ion batteries. Specifically, we have constructed and characterized ultra-thick graphite electrodes using 3D Cu foam as current collectors. Cu foam electrodes are as thick as 1.2 mm, about ten times the thickness of conventional lithium ion electrodes. Although high rate performance remains very challenging, the electrode exhibits very good storage capability and cycling stability at rates lower than C/5 rate. We have also designed a bipolar configuration cell to study the effects of thickness on the electrochemical performance of the ultra-thick Cu foam electrodes. For the 3 thicknesses (1.2, 0.6, and 0.3 mm) investigated, both 0.6 and 0.3 mm thick electrode showed good capacity retention up to a C/5 rate. Furthermore, we have constructed a 1.2 mm thick Al foam electrode with L333 as a cathode material. A full cell was assembled by combining the Cu foam graphite negative and Al foam L333 positive electrodes. Very good charge storage capacity and cycling stability were observed up to C/5 rates.

In summary, we have shown that a full cell composed of two ultra-thick foam electrodes offers good charge storage capacity and cycling stability at low rates. The material loading (thickness) of the electrodes are more than 10 times those of the current SOA batteries. However, at higher rates, resistance and kinetic issues are noticeable. Prior report also suggests that ionic conductivity could also be a limiting factor for thick electrodes [24]. While further research is needed to determine the electronic and ionic conductivity limitations of the thick electrodes at higher rates, we believe these losses can be significantly improved by tuning the 3D architectures by addressing the pore size, porosity, and surface area of the foam structures. Our results confirm that 3D structured foam current collectors enable ultra-thick battery electrodes and provide a promising approach to improve the utilization of active materials for high energy battery applications.

References

[1] M. Armand, J.M. Tarascon, Nature 451 (2008) 652.
[2] J.M. Tarascon, M. Armand, Nature 414 (2001) 359.
[3] USABC test procedures at http://www.uscar.org/guest/teams/12/U-S-Advanced-Battery-Consortium.
[4] P.L. Taberna, S. Mitra, P. Poizot, P. Simon, J.M. Tarascon, Nat. Mater. 5 (2006) 567.
[5] M.M. Shaijumon, E. Perre, B. Daffos, P.L. Taberna, J.M. Tarascon, P. Simon, Adv. Mater 22 (2010) 4978.
[6] P. Hiralal, S. Imaizumi, H.E. Unalan, H. Matsumoto, M. Minagawa, M. Rouvala, A. Tanioka, G.A.J. Amaratunga, ACS Nano 4 (2010) 2730.
[7] W. Yao, J. Chen, H. Cheng, J. Solid State Electrochem. 15 (2010) 1597.
[8] W. Wang, P.N. Kumta, ACS Nano 4 (2010) 2233.
[9] C.R. Sides, X. Fan, C.R. Martin, ECS Trans. (2006) 13.
[10] Y.S. Kim, H.J. Ahn, S.H. Nam, S.H. Lee, H.S. Shim, W.B. Kim, Appl. Phys. Lett. 93 (2008).
[11] H. Zhang, G. Cao, Z. Wang, Y. Yang, Z. Shi, Z. Gu, Electrochem. Commun. 10 (2008) 1056.
[12] L. Dimesso, S. Jacke, C. Spanheimer, W. Jaegermann, J. Alloys Compd 509 (2011) 3777.
[13] G. Oltean, L. Nyholm, K. EdstrÃm, Electrochim. Acta 56 (2011) 3203.
[14] S. Zhang, Y. Xing, T. Jiang, Z. Du, F. Li, L. He, W. Liu, J. Power Sources 196 (2011) 6915.
[15] S.K. Cheah, E. Perre, M. Rooth, M. Fondell, A. HÃ¥rsta, L. Nyholm, M. Boman, T. Gustafsson, J. Lu, P. Simon, K. EdstrÃm, Nano Lett. 9 (2009) 3230.
[16] T. Jiang, S. Zhang, X. Qiu, W. Zhu, L. Chen, J. Power Sources 166 (2007) 503.
[17] L. Bazin, S. Mitra, P.L. Taberna, P. Poizot, M. Gressier, M.J. Menu, A. Barnab, Ã.P. Simon, J.M. Tarascon, J. Power Sources 188 (2009) 578.
[18] X. Xiao, P. Liu, J.S. Wang, M.W. Verbrugge, M.P. Balogh, Electrochem. Commun. 13 (2011) 209.
[19] J.M. Boulton, G.M. Cintra, K.S. Nanjundaswamy, A. Kaplan, Battery Electrodes and Batteries Including Such Electrodes (US20080241664).
[20] G. Che, B.B. Lakshmi, E.R. Fisher, C.R. Martin, Nature 393 (1998) 346.
[21] C.R. Sides, N. Li, C.J. Patrissi, B. Scrosati, C.R. Martin, MRS Bull. 27 (2002) 604.
[22] H. Zhang, X. Yu, P.V. Braun, Nat. Nano (2011) (advance online publication).
[23] M. Winter, J.O. Besenhard, M.E. Spahr, P. Novák, Adv. Mater. 10 (1998) 725.
[24] C. Fongy, A.C. Gaillot, S. Jouanneau, D. Guyomard, B. Lestriezb, J. Electrochem. Soc. 157 (7) (2010) A885.